JOURNAL OF VIROLOGY, Aug. 1997, p. 5849–5860 Vol. 71, No. 8
0022-538X/97/$04.00+0

Selection of a Nonconsensus Branch Point Is Influenced by an RNA Stem-Loop Structure and Is Important To Confer Stability to the Herpes Simplex Virus 2-Kilobase Latency-Associated Transcript

CLAUDE KRUMMENACHER,† JANICE M. ZABOLOTNY, AND NIGEL W. FRASER*
The Wistar Institute, Philadelphia, Pennsylvania 19104-4268

Received 27 February 1997/Accepted 25 April 1997

Herpes simplex virus type 1 latent infection in sensory neurons is characterized by the highly restricted transcription of viral genes. The latency-associated transcripts (LAT) family members are the only transcripts that can be identified in large amounts in latently infected cells. The most abundant LAT species is a 2-kb RNA that results from splicing of a rare primary transcript. Analysis of a LAT mutant virus (TB1) in cell culture revealed an aberrant splicing pattern and production of a stable small (0.95-kb) LAT intron. A panel of deletion constructs expressing truncated LAT in transiently transfected cells mapped the region influencing stability to the 3′ end of the LAT intron. This region encompasses the branch point and a putative stable stem-loop hairpin structure immediately upstream of the splice acceptor consensus polypyrimidine tract. Mutagenic analysis of the sequence in this region confirmed our hypothesis that the stem-loop structure is important for efficient splicing by influencing the selection of a nonconsensus branch point. Changes in this structure correlate with changes in branch point selection and production of an unstable 2-kb LAT.

Herpes simplex virus type 1 (HSV-1) is a human pathogen that causes lifelong infection punctuated with recurrent episodes of massive viral production (56). After an initial acute infection of the mucosa, HSV-1 infects nerve endings and travels to sensory ganglia, where it can establish a latent infection in neurons (38). Upon stress, the viral genome undergoes extensive transcription and replication, leading to the production of viral proteins and infectious particles (18, 51). In contrast to the initial acute infection or subsequent reactivation, the latent stage is characterized by a tight transcriptional repression of all classes of viral genes, with the exception of a diploid locus in the long repeat elements known as the latency-associated transcript (LAT) gene (9, 44, 52). The most abundant LAT species is a 2-kb nonpolyadenylated transcript referred to as the 2-kb LAT (44, 50, 52). Removal of a short intron in the 2-kb LAT leads to the production of a small variant of 1.5 kb (47). This smaller LAT is observed only during latency in neurons, whereas the 2-kb LAT is also expressed during productive infection with late gene kinetics (46, 55). The primary LAT transcript, known as the minor LAT species (mLAT), extends for 8.3 kb from the main LAT promoter to the first downstream polyadenylation signal (29; reviewed in reference 17).

The role of the LAT gene products during the life cycle of HSV is not clearly understood. Since they are expressed during the latent phase of infection, their role in the establishment and maintenance of and reactivation from latency has been examined. Some HSV-1 LAT-negative viruses display limited efficiency in establishing latency in neurons (41) and/or reduced reactivation kinetics in animal models (3, 5, 22, 26, 33, 53). The large number of overlapping genes (ICP0, ICP4, and γ-34.5) and other newly described transcripts (ORF P, ORF O, and LS/Ts) in this region often prevents a direct assignment of the observed phenotype to LAT; indeed, the functional LAT gene products are not precisely defined. Despite much effort (13), and in contrast to findings with bovine herpesvirus (42), no functional LAT-derived protein has been clearly identified. Since the 2-kb LAT accumulates to high levels in infected neurons, it is thought by many to be an active RNA. However, the mechanism of synthesis for this LAT transcript and its function remain elusive. Since it is partially complementary to the 3′ end of the ICP0 mRNA, the 2-kb LAT has been proposed to be involved in an antisense suppression mechanism (16, 52).

The 2-kb LAT, beginning some 600 bp downstream of the main LAT promoter (12, 59) and lacking most of the structural characteristics of an mRNA such as a cap or poly(A) tail (11, 54), has been postulated to be a stable intron accumulating after splicing of the minor LAT (mLAT) (12). The ability of the 2-kb LAT sequence to be excised from a β-galactosidase mRNA was first demonstrated experimentally by Farrell et al. (16). Recent structural data reporting the nonlinear nature of both the 1.5- and 2-kb LATs (37, 57) and mapping of the branch point of this RNA (58) confirmed the intronic origin of the 2-kb LAT.

In the course of natural RNA processing, introns are removed from mRNA by a succession of molecular events involving specialized factors such as small nuclear ribonucleoproteins (30). Proper recognition of splicing signals, such as splice donor and acceptor sites, and branch point sequences by small nuclear RNPs are essential steps in this process (19, 35). Consensus branch sites are efficiently selected, whereas nonconserved sites are poorly recognized and often lead to suboptimal alternative splicing (48) or exon skipping (21, 25, 36). In addition to the branch point itself, surrounding regions (7, 14), RNA secondary structures (15, 20, 43), and polypyrimidine tract sequences (32, 39) are known to influence branch point selection. Introns are usually rapidly degraded by a mul-

* Corresponding author. Mailing address: The Wistar Institute, 3601 Spruce St., Philadelphia, PA 19104-4268. Phone: (215) 898-3847. Fax: (215) 898-3849. E-mail: fraser@wista.wistar.upenn.edu.
† Present address: Department of Microbiology, School of Dental Medicine, University of Pennsylvania, Philadelphia, PA 19104-6002.

tistep process involving nucleases and specialized debranching enzymes (1, 30, 31). The 2-kb LAT intron has been reported to be more resistant to the action of debranching enzymes (37). Other stable introns of cellular (34) and viral (6) origin have been described. A general mechanism underlying intron resistance to degradation, however, has not been elucidated. Different strategies have evolved to confer stability to RNA, particularly to mRNA. These include (i) secondary structures serving as protein-docking sites, (ii) the presence of a long polyadenylated tail, and (iii) possible sequestration in a nuclease-free environment (40).

In this study we investigated the sequence requirements for the production of a stable 2-kb LAT in tissue culture. On the basis of observations from an HSV-1 LAT mutant producing a truncated LAT intron (4) and a panel of mutated LAT expression plasmids, we mapped a region at the 3′ end of the 2-kb LAT which is important for stability. The nucleotide sequence involved in the formation of a putative secondary structure in the tail of the 2-kb LAT lariat was found to be responsible for nonconventional branch point selection, influencing both splicing efficiency and stability of the intron.

MATERIALS AND METHODS

Cells and virus. Cos-1 cells were grown in Iscove's medium supplemented with 5% calf serum. CV-1 cells were maintained in Eagle's minimal essential medium plus 5% calf serum. HSV-1 mutant TB1 and HSV-1 F were prepared as previously described (4, 9, 10).

Plasmid construction. The 2.8-kb *Pst*I-*Mlu*I restriction fragment encompassing the LAT gene of HSV-1 F was subcloned into the *Eco*RI and *Hin*dIII sites of pcDNA3 (Invitrogen) as described previously (58). The resulting plasmid, pcDNA3Pst-Mlu, served as the backbone for subsequent mutations and will be referred as the wild-type (wt) plasmid. Mutants pΔHpa and pΔXcm were generated by removal of the corresponding restriction fragment and self-ligation (prior Klenow filling in was necessary in the case of pΔXcm). To construct pΔBfa, the 2.8-kb *Eco*RI-*Hin*dIII fragment from pcDNA3Pst-Mlu was isolated and digested with *Bfa*I. The resulting 2,110-bp *Hin*dIII-*Bfa*I and 400-bp *Bfa*I-*Eco*RI fragments were purified and ligated directly in the *Eco*RI-*ind*III-digested wt vector. Plasmids pHλ+ and pHλ− were generated by the insertion in pΔHpa of the 440-bp *Hpa*I fragment consisting of lambda phage DNA from plasmid pNF1. In pHλ−, the phage DNA insert is in the same orientation as in the TB1 virus; it is in the opposite orientation in pHλ+.

The pBam clone was generated by site-directed mutagenesis (23) to create a unique *Bam*HI site toward the 3′ end of the 2-kb LAT. Fragments from pcDNA3Pst-Mlu were amplified by PCR with primers PFPML (GGGGCATC ACGTGGTTACCC) and PRBAM (GAGACAAGAGGAAGGATCCCTCG GC) or with PFBH1 (AGGGATCCTTCCTCTTGTCTCCCTCCCAGG) and PRP31 (GCCAGTGTGATGGATATCTGC). Both amplified products were purified from agarose gels and mixed equally in a second PCR with PFPML and PRP31 as amplification primers. The 700-bp final product was digested with *Eco*RI and *Bbr*PI (*Pml*I) and cloned into the corresponding sites of vector pcDNA3Pst-Mlu. Following the same procedure, pCons was generated with pCR primers PRPB10 (GGAAAGGTCAGTGGGCCCCCGCGCTGCTTCTGG) plus PFPML and PFPB9 (CACTGACCTTTCCTCTTGTCTCCCTCCCAGG) plus PRP31 in the first-step PCR amplifications.

Mutant pY+ was generated by the insertion of a linker (GATCGTACTAAC) containing the yeast consensus branch point sequence into the *Bam*HI site of pBam. In pY−, the same linker was inserted in the opposite orientation (GAT CGTTAGTAC). Plasmid pΔPB was obtained after removal of the *Pml*I-*Bam*HI fragment from pBam, Klenow filling in, and self-ligation of the plasmid. To generate plasmids pΔ1, pΔ2, and pΔ3, DNA from wt vector was amplified by PCR with, respectively, PFPB1 (CCACACGTGAGACCCCCGAGATGGGC AGG), PFPB2 (CGCCACGTGGGACGGCCCCGGAAGTCTCC), PFPB3 (TT CCACGTGCCCCGCGGCCCAGAAGCAGC), and PRP31; the fragments were gel purified, digested with *Eco*RI and *Pml*I, and cloned into the corresponding sites of pcDNA3Pst-Mlu. To obtain pΔ4, DNA from pcDNA3Pst-Mlu was amplified with PRPB6 (GGAAACCTCCCTCCCGAGGAAGTGTGCCCGGAAG ACG) and PFPML or with PFPB7 (GAGGGAGGTTTCCTCTTGTCTCCCTC CCAGG) and PRP31; amplified fragments were gel purified and equally mixed in a PCR with PFPML and PRP31 as primers. The final product was digested with *Pml*I and *Eco*RI and cloned into the corresponding sites of the wt vector. Mutant pΔ5 was generated by the same method but with PRPB6 replaced by PRPB8 (GGAAACCTCCCTCCCGCGGGCGGCCTCACGCGCTACC). Mutant pΔG was engineered in the same way with primers PFDBG (CGTGGCG CGTCTTACACTTCCTCGGCCC) and PRP31 or primers PFPML and PRDBC (AAGACGCGCCACGCGGAGGC). The resulting products were gel purified and mixed in a second amplification reaction with primers PFPML and PRP31. The final 700-bp product was purified, digested with *Pml*I and *Eco*RI, and cloned in the corresponding sites of pΔ3. A similar procedure was used for pΔA with primers pFDELA (CAGCGCCGGGGCCTTTCCTCTTGTCTCCCTCCCAGG) and PRDELT (AAAGGCCCCGGCGCTGCTTCTGG) in the first-step PCRs.

All amplification reactions were performed under the same conditions: 35 cycles of 1 min at 94°C, 1 min at 60°C (58°C), and 1 min at 72°C in 1× PCR buffer [60 mM Tris-HCl (pH 9.5), 15 mM $(NH_4)_2SO_4$, 1.5 to 2.0 mM $MgCl_2$]–0.2 mM deoxynucleoside triphosphates–1 μM each oligonucleotide–0.5 U of *Taq* polymerase (Fisher Scientific). Five cycles with an annealing temperature of 58°C were performed in the absence of oligonucleostides prior to standard amplification in the second-step PCR when two PCR fragments had to be linked as the template.

Transfection and RNA extraction. A 20-μg portion of plasmid per 10-cm dish was transfected into subconfluent Cos-1 cell monolayers by calcium phosphate precipitation (2). The cells were left with the precipitate for 16 h, shocked in phosphate-buffered saline–15% glycerol for 2 min, washed with phosphate-buffered saline, and incubated for 22 to 24 h at 37°C. Alternatively, subconfluent CV-1 cells were infected with 1 PFU of TB1 or HSV-1 F virus per cell. RNA was isolated 16 h postinfection. Transfected or infected cells were lysed in 3.5 ml of lysis buffer (4 M guanidine isothiocyanate, 0.5% sodium *N*-lauroylsarcosine, 100 mM β-mercaptoethanol, 25 mM sodium citrate [pH 7.0], 0.1% antifoam A). DNA was sheared for 10 s by a mechanical disrupter (Brinkmann Instrument Inc.). Total RNA was pelleted through a cushion of 5.7 M CsCl–0.1 M EDTA by centrifugation at 150,000 × *g* for 20 h at 18°C. The RNA pellet was resuspended in H_2O and precipitated with ethanol. RNA was stored in ethanol at −70°C.

Northern blot analysis. RNA was resuspended in H_2O, and the absorbance at 260 nm was measured spectrophotometrically. A 5-μg portion of total RNA was treated with glyoxyal, separated on a 1.2% agarose gel, and transferred on GeneScreen Plus (NEN) membrane as previously described (45). The filters were prehybridized for 2 h at 50°C in 50% formamide–10% dextran sulfate–1× Denhardt's solution–1% sodium dodecyl sulfate–5× SSC (1× SSC is 0.15 M NaCl plus 0.015 M sodium citrate)–1 mM EDTA–0.1% denatured salmon sperm DNA. The ^{32}P-labeled nick-translated probe was heat denatured, added to the prehybridization mix, and incubated overnight at 50°C. The blots were washed in decreasing concentrations of SSPE (1×, 0.5×, and 0.1×) (1× SSPE is 0.18 M NaCl, 10 mM NaH_2PO_4, and 1 mM EDTA [pH 7.7])–1% SDS at 65°C, twice for 20 min per wash, and exposed on a PhosphorImager screen (Molecular Dynamics). The bands were quantified with ImageQuant version 1.1 software.

RT-PCR. To characterize the splice junctions of LAT, cDNA was synthesized from 1 μg of DNase-treated total RNA with the Superscript II preamplification kit (Gibco BRL). The manufacturer's protocol for high GC content RNA was followed with the use of both poly(dT) and random hexanucleotides as primers. PCR was performed on 20 ng of cDNA with 1 μM primers exon1 (GCTCCAT CGCCTTTCCTGTT) and exon2N (TCCTCTGCCTCTTCCTCCTCG) in 1× PCR buffer–0.2 mM deoxynucleoside triphosphates–0.5 U of *Taq* polymerase (Fisher Scientific) in a 50-μl reaction volume. The conditions of the 35 amplification cycles were 1 min at 94°C, 1 min at 60°C, and 1 min at 72°C. A 5-μl sample of the reaction product was electrophoresed on a 2% agarose gel and visualized by ethidium bromide staining. Amplified bands were extracted from the gel with a Geneclean kit (Bio 101, Inc.), cloned into a TA vector (Invitrogen), and sequenced with an ABI Prism cycle sequencer.

To map the branch point of the different introns, reverse transcription-PCR was performed as described previously (58). Briefly, LAT-specific cDNA was synthesized from 10 μg of DNase-treated total RNA with the "branch" oligonucleotide (AGAAGCAGGTGTCTAACCTACNNN) as primer. This cDNA was subjected to a PCR amplification performed with primers PFPML (GGGG CATCACGTGGTTACCC) and PREND (AGAAGCAGGTGTCTAACCTA C). The PCR products were isolated from 2% agarose gels, cloned into a TA vector (Invitrogen), and sequenced.

RESULTS

Production of altered LAT after insertion of a lambda sequence in the 2-kb LAT. The HSV-1 insertion mutant TB1, which has a 168-nucleotide deletion in the middle of the 2-kb LAT region replaced by 440 nucleotides of lambda phage DNA, has been shown to be unable to express a stable 2-kb LAT in lytically infected cells or latently infected animals (4). To determine the mechanism underlying this particular phenotype, a LAT-expressing plasmid vector was constructed in which the TB1 mutation was re-created. In the parental vector, a 2.8-kb *Pst*I-*Mlu*I fragment encompassing the 2-kb LAT of HSV-1 F is expressed under the control of a cytomegalovirus immediate-early promoter. The bovine growth hormone polyadenylation signal is present downstream of the HSV-1 insert, ensuring proper termination of transcription. We have previously identified the three transcripts expressed by this plasmid as a truncated mLAT primary transcript (3.4 kb), the 2-kb LAT

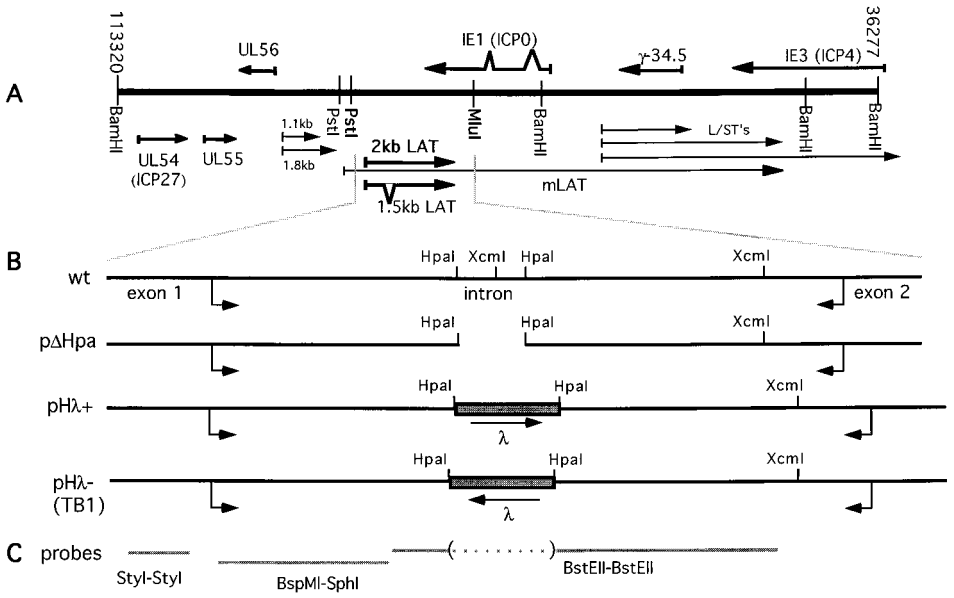

FIG. 1. Schematic representation of the LAT locus of HSV-1. (A) Genomic *Bam*HI restriction fragments B, SP, and Y are represented, as well as transcripts arising from this region (arrows). Nucleotides are numbered by the convention of McGeoch et al. (28). (B) The 2.8-kb *Pst*I-*Mlu*I fragment containing the 2-kb LAT cloned in pcDNA3 (Invitrogen) is enlarged (wt). Arrows represent the splice donor and acceptor sites at the beginning and end of the wt 2-kb LAT. The 168-bp deletion in the construct pΔHpa is also shown. The shaded boxes represent the λ phage DNA sequences, with arrows indicating their orientations in both pHλ+ and pHλ− constructs. (C) The different probes used in Northern blots are shown as gray lines. The upstream *Sty*I-*Sty*I probe is specific for exon 1. Probe *Bsp*MI-*Sph*I covers the 5′ end of the 2-kb LAT upstream of the λ insert. Probe *Bst*EII-*Bst*EII covers most of the 3′ end of the 2-kb LAT and the missing *Hpa*I fragment and extends 210 nucleotides upstream of the 5′ *Hpa*I site.

intron, and spliced exons of mLAT (1.4 kb) (58). In this wt construct, the TB1 mutation was engineered by replacing the 168-bp *Hpa*I-*Hpa*I fragment with a 440-bp sequence of lambda phage DNA digested with *Hpa*I to yield the clone pHλ−. As controls, the same LAT fragment was deleted in pΔHpa or replaced with the phage sequence in the reverse orientation in pHλ+ (Fig. 1).

After transfection of these constructs in Cos-1 cells, total RNA was extracted and subjected to Northern blot analysis as described in Materials and Methods. Three nonoverlapping probes designed to detect either the intron or the first exon were used to map the different transcripts from the LAT locus (Fig. 1). The first of these probes (Fig. 2A) was specific for the 5′ end of the 2-kb LAT intron, upstream of the lambda phage insert. This probe detected the normal 2-kb LAT expressed by the wt construct (Fig. 2, lane 1). When cells were transfected with pΔHpa or pHλ+, the accumulated intron was also visible, although with a different size corresponding to the deletion or insertion (lanes 2 and 4). However, in the case of the TB1-like mutant pHλ−, no LAT RNA was detected by this probe (lane 3). All the probes used could potentially detect the 3.4-kb primary transcript starting at the cytomegalovirus promoter and ending at the polyadenylation signal (58). This longer transcript was present in very small amounts, suggesting a very efficient splicing, and did not always appear on the blots after a short exposure following hybridization with specific probes.

The RNA described above was hybridized with a second probe, which was able to detect the 3′ end of the 2-kb intron downstream of the λ phage sequence insert (Fig. 2B). The wild-type 2-kb LAT (Fig. 2, lane 5), as well as introns from pΔHpa and pHλ+, could also be detected by this probe (Fig. 2, lanes 6 and 8). In the case of pHλ−, a smaller RNA of about 1 kb was detected (lane 7). Similarly, a transcript with the same size was produced following infection of CV-1 cells with the TB1 virus (lane 9) (4). With the 3′ intronic probe, low levels of primary transcripts were detected following transfection of the different constructs (lanes 5 to 8); however, no band indicating such a transcript could be detected following infection with TB1 (lane 9). A very faint smear at a high molecular weight could be detected, possibly due to probe hybridization with genomic HSV-1 DNA. The location of a polyadenylation sig-

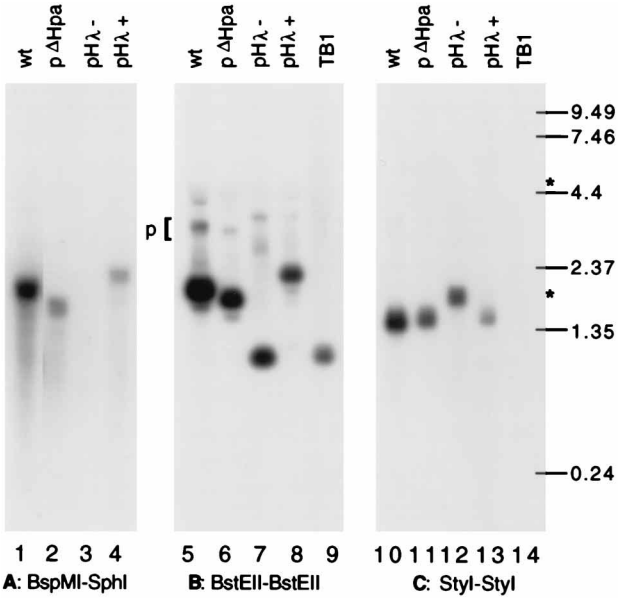

FIG. 2. Northern blot analysis of LAT RNA. Cos-1 cells were transfected with LAT-expressing vectors (wt, pΔHpa, pHλ−, and pHλ+). Alternatively, CV-1 cells were infected with TB1 virus, and RNA was collected 16 h postinfection. Total RNA was collected after 40 h, and 5 μg was electrophoresed and blotted. The three different probes used for hybridization are indicated under the blots. The RNA was probed with a 0.59-kb *Bsp*MI-*Sph*I fragment specific for the 5′ region of the 2-kb LAT (A), a 1-kb *Bst*EII-*Bst*EII probe specific for the 3′ and 5′ regions of the 2-kb LAT (B), and a 0.37-kb *Sty*I-*Sty*I fragment upstream of the 2-kb LAT (C). p indicates the primary transcripts. Molecular size markers (in kilobases) are indicated on the left. Asterisks represent the positions of 28S and 18S rRNAs.

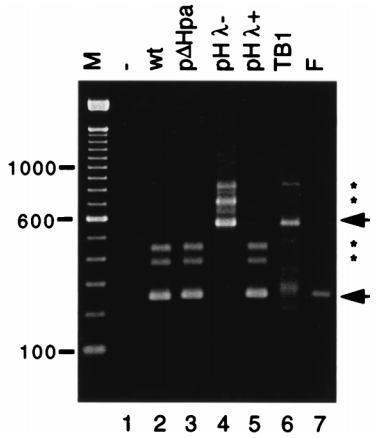

FIG. 3. RT-PCR of spliced LAT RNA. Total RNA from Cos-1 cells was collected 40 h after transfection with the different constructs (wt, pΔHpa, pHλ−, and pHλ+). RNA from CV-1 cells was harvested 16 h after infection with HSV-1 F (F) or the HSV-1 TB1 mutant (TB1). A 1-μg portion was subjected to DNase treatment and reverse transcribed into cDNA. The equivalent of 20 ng was used as template for PCR with primers exon1 and exon2N. The major bands of 245 bp (lanes 2, 3, 5, and 7) and 550 bp (lanes 4 and 6) are indicated by arrows. Additional bands in transfection experiments are indicated by asterisks. No fragments were amplified from cellular cDNA (data not shown) or when cDNA was omitted (lane 1). None of these bands were observed in the absence of RT (data not shown).

nal relatively close to the end of the intron in the cloning vector allows easier detection of the truncated mLAT compared to the viral mLAT. This may be due to greater homogeneity or greater stability of this shortened primary transcript.

Finally, the RNA was hybridized with a probe specific for exon 1 of the LAT without overlapping the 2-kb intron (Fig. 2C). Spliced exons of the expected size (1.4 kb) were produced after excision of the 2-kb LAT from the primary transcript (Fig. 2, lane 10). Deletion of the *Hpa*I region (lane 11) or insertion of the lambda phage sequence in the pHλ+ construct (lane 13) did not affect the production or the size of the mature exons. However, after transfection of pHλ− (lane 12), the mature RNA produced was 0.4 kb larger than the wt transcript. In contrast, no detectable amount of transcripts containing the first exon was found in TB1-infected cell RNA (lane 13). This reflects the extremely low abundance of both viral primary transcripts (mLAT) and mature LAT transcripts following HSV-1 infection with the TB1 mutant.

The expression of the TB1-like mutated LAT in transient-transfection assays indicated that LAT was made in the TB1-homolog construct as it is made by the TB1 virus. Although primary transcripts or mature RNA could not be observed, the presence of an RNA mapping to the 3′ end of the 2-kb LAT intron reflected transcription in the LAT locus in both infected and transfected cells. However, the mutant differed from the wt because the orientation-dependent insertion of the lambda phage sequence strongly affected the splicing of the LAT primary transcript.

Alternative splicing of the mutant TB1 2-kb LAT. To further characterize the LATs in the TB1 mutant virus, mapping of the splice donors and acceptors was performed by RT-PCR on RNA from transiently transfected or infected cells. The forward primer (exon1) was located in exon 1, and the reverse primer (exon2N) was located after the end of the 2-kb LAT (see Fig. 4). Following amplification, a 245-bp fragment could be detected if the 2-kb sequence was excised, whereas no cDNA was amplified if the primary transcript was used as the template. After infection of CV-1 cells with HSV-1 F, the 245-bp product was detected (Fig. 3, lane 7). The same band was observed following expression of LAT cloned in wt, pΔHpa, and pHλ+ plasmid constructs (lanes 2, 3, and 5). The higher-molecular-weight bands of cDNA following transfections correspond to alternatively spliced RNAs resulting from the vector expression system and may not be biologically relevant for the virus (58). For both TB1 virus infection and pHλ− plasmid construct transfection, a larger PCR product was observed (lanes 4 and 6). This finding is consistent with the size of the mature exons detected by Northern blotting (Fig. 2). In that case, the heterogeneity of the RT-PCR product, although more prevalent after transfection, was observed to a lesser extent when the cells were infected with TB1 (Fig. 3, compare lanes 4 and 6). The detection of TB1 LAT cDNA with primers specific to sequences in the first and the second LAT exons confirmed the presence of a mature spliced transcript. These results suggest that a LAT unspliced primary transcript and a spliced mature RNA, though altered, are produced by TB1 during productive infection and also that the mutation in TB1 does not affect directly transcription from the LAT promoter.

Major products of the RT-PCR were extracted from agarose gels (Fig. 3) and cloned. A number of representative clones were sequenced, and the more abundant splicing products are depicted in Fig. 4. The wt viral transcript (TRwt), whose splicing leads to the production of the 2-kb LAT, is shown, as well as an alternatively spliced transcript (TRwt1) that is present only after transient transfection of the wt plasmid. The transcript (TR1) was the most abundant in pHλ−-transfected cells and TB1-infected cells. Other minor transcripts, TR2 and TR3 (all larger than TR1), were detected in transiently transfected cells. Although they were overrepresented in the transfection assay and might be irrelevant for the virus, these transcripts (TRwt1, TR2, and TR3) indicated that known neuron-specific (SD_N, SA_N) and cryptic (SA*) splice sites could be used in nonneuronal cells during LAT splicing. Interestingly, in all altered LATs from TB1 or pHλ−, the 945-bp downstream intron was always conserved, as well as the splice donor site in the lambda sequence (GCAG-GTAA) at position 418 of the insert. In contrast, the lambda-specific splice acceptor site

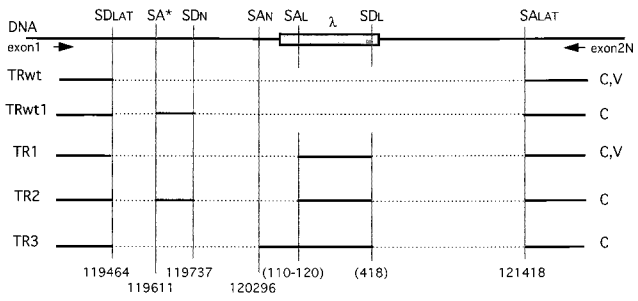

FIG. 4. Map of LAT transcripts from the TB1 virus and pHλ− construct. The first line represents the genomic LAT locus in TB1 and pHλ−. The shaded box represents the λ DNA insert. SD_{LAT} and SA_{LAT} indicate the splice donor and acceptor sites, respectively, used in HSV-1 and in the wt construct to generate the 2-kb LAT intron. SD_N and SA_N show the splice sites used to generate the 1.5-kb LAT during latency in neurons (47). SD_L and SA_L indicate the sites acting as splice donor and acceptor in the lambda sequence. SA* localizes a cryptic splice acceptor site in the 2-kb LAT. Nucleotide positions on the HSV-1 genome refer to those of McGeoch et al. (28). Different transcripts (TR) identified after RT-PCR with primers exon1 and exon2N (arrows) are represented with exons as solid lines and introns as dotted lines. TRwt shows the wt transcript from construct "wt" (C) and HSV-1 strain F (V). TRwt1 is a transcript produced only after transfection of the wt construct (C). TR1, TR2, and TR3 are transcripts from the pHλ− construct (C) and/or TB1 virus (V).

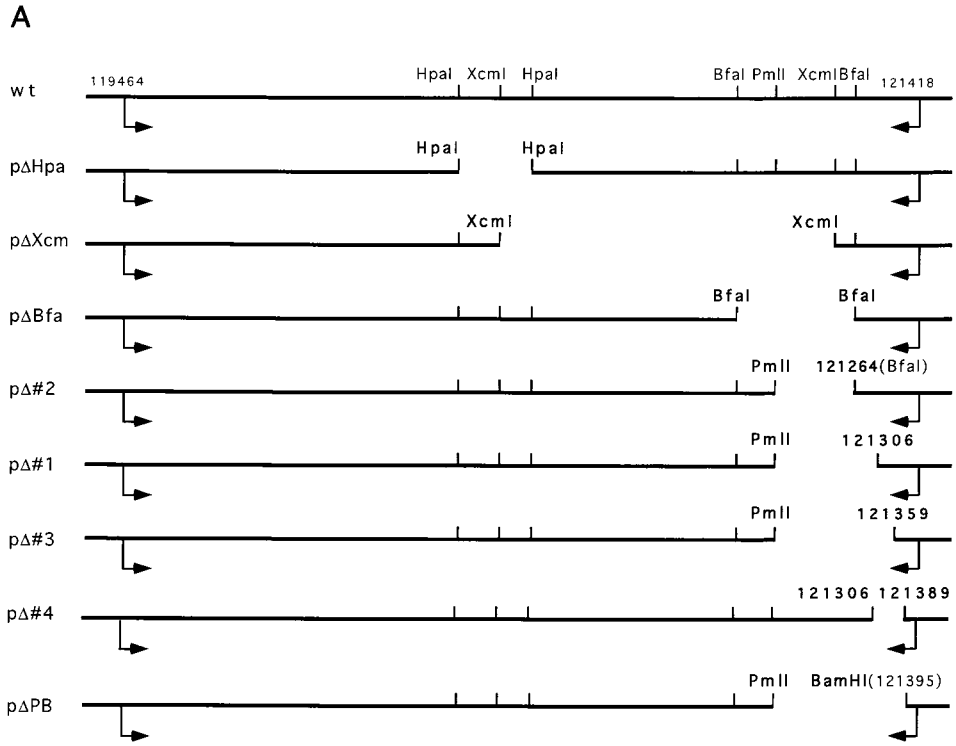

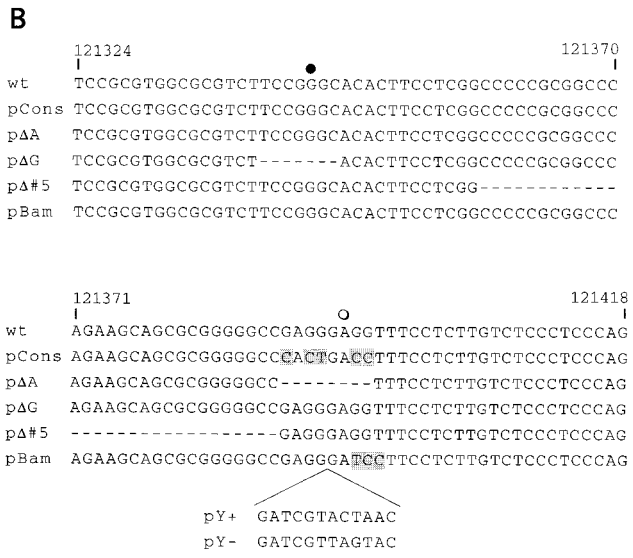

FIG. 5. Map of mutations. (A) The 2-kb LAT region with splice donor and splice acceptor sites (arrows) is shown for each construct. The relevant restriction sites are indicated. (B) Detailed map of the last 95 nucleotides of the 2-kb LAT with smaller deletions (dashes) or substitutions (gray boxes). pY+ and pY− are identified by the insertion they carry in the *Bam*HI site of pBam. The solid circle indicates the branch nucleotide of LAT identified by Zabolotny et al. (58), and the open circle shows the putative branch point hypothesized by Wu et al. (57). Nucleotides are numbered by the convention of McGeoch et al. (28).

(SA_L) appeared to be less highly conserved and varied between positions 110 and 120 of the lambda sequence.

Elucidation of the sequence of these mature transcripts, together with the Northern analysis, showed that the insert of phage DNA in TB1 resulted in the addition of a splice donor and a splice acceptor site in the middle of the 2-kb LAT intron. The resulting mature transcript contained an additional exon made of lambda-derived RNA. The LAT intron upstream of this new lambda exon did not accumulate and was not detected by Northern blotting (Fig. 2A). In contrast, the downstream 0.95-kb LAT intron could be seen on Northern blots (Fig. 2B), indicating its remarkable stability similar to full-length 2-kb LAT.

Mapping the stability determinant to the 3′ end of 2-kb LAT. On the basis of the TB1 virus and the pHλ− construct, it appeared that the determinant for stability of the LAT intron resides in the 3′ half of 2-kb LAT. To map this region more precisely, series of deletions covering the region downstream of the *Hpa*I sites were engineered in the same plasmid expression system used previously (Fig. 5A). Vectors expressing LAT deletion mutants were transiently transfected in Cos-1 cells, and LAT RNA was analyzed by Northern blotting, as shown in Fig. 6A. The probe specifically detected the 5′ half of the 2-kb LAT intron in a region not affected by deletions in any of the mutants. The 2-kb intron was expressed following transfection of the wt construct (Fig. 6, lane 1), whereas no hybridization was visible in nontransfected Cos-1 cells (lane 10). For all but two of these mutants, the presence of a stable but variable-sized intron due to the deletion was detected (lanes 2 to 6 and 9). Deletions Δ3 and ΔPB affected the accumulation of intron, although small amounts of primary transcript could be detected as for all the other constructs. The absence of visible intron from these constructs could be due to inefficient transcription, a defect in splicing, or rapid degradation of an unstable intron.

To clarify this point, the same blot was rehybridized with a probe specific for the LAT exon 1 (Fig. 6B). For all transfected constructs, a band corresponding to the mature transcript with completely spliced exons (1.4 kb) was detected. This indicated that in all cases, transcription and splicing of LAT occurred

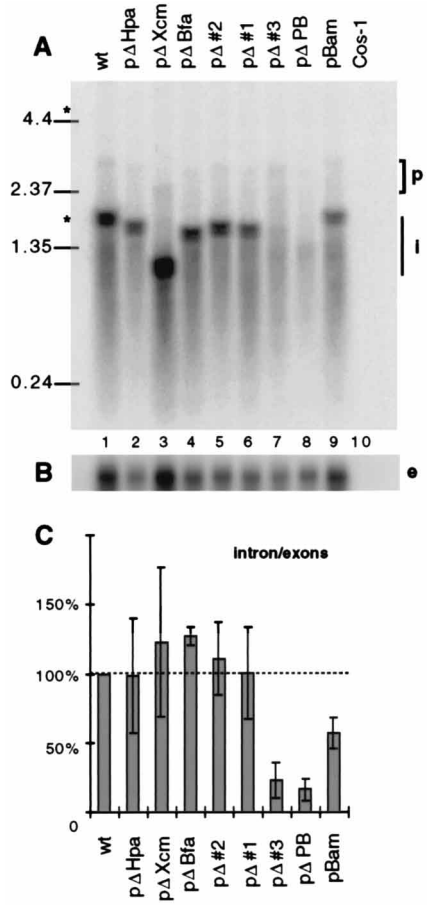

FIG. 6. (A) Northern blot of the LAT intron. A 5-μg portion of RNA from Cos-1 cells harvested 40 h after transfection with the wt (lane 1) or mutated (lanes 2 to 8) plasmid constructs. Nontransfected Cos-1 cell RNA was loaded on lane 10. The *Bsp*MI-*Sph*I probe was specific for the 3′ region of the 2-kb intron. Positions of molecular size markers (in kilobases) are indicated on the left. Asterisks show the positions of 28S and 18S rRNAs; p represents the low-abundance LAT primary transcript; i indicates the introns produced by the different mutants. (B) The same blot was reprobed with the *Sty*I-*Sty*I probe specific for exon 1 of LAT. The spliced exon 1.4-kb band resulting from splicing is shown (e). (C) The intron band from panel A and exon band from panel B were quantified for each mutant in this experiment, as well as in two other independent transfection experiments. The ratio of intron to exons is represented in the histogram. This ratio was normalized to 100% for the wt construct (dotted line) in each of the experiments, and the ratio for each mutant was calculated relative to this standard. Error bars represent ±1 standard deviation.

without major recombinations or alterations as reported for TB1. To understand the effects of these deletions more precisely, the stability of the intron was quantified with a PhosphorImager to measure the intensity of each band. The relative stability of the intron was assessed by calculating the ratio of intron over exons for each mutant. This approach eliminates artifacts due to differences in transfection efficiency, transcriptional levels, or amounts of RNA loaded in each well, because introns and exons are produced at the same rate in any mutant. Since spliced exons are similar in all constructs, their stability is assumed to be the same regardless of the mutation affecting the intron; therefore, a difference in ratio is a measure of intron stability. A quantification from three independent transfection experiments is summarized in Fig. 6C. To compare the results from different experiments quantitatively, the result obtained with the wt construct was normalized to 100% in each experiment and represented the standard stability of the 2-kb LAT intron. The deletions ΔHpa, ΔXcm, ΔBfa, Δ2, and Δ1 did not significantly alter LAT stability, confirming the direct observation of the Northern blot analysis. In contrast, pΔ3 and pΔPB showed a marked reduction in stability to about 10% of that of the wt 2-kb LAT—a value close to background. Interestingly, the pBam mutant, which carries only a 3-base substitution (Fig. 5B), showed a stability reduced to 60% of that of the wt (Fig. 6, lane 9). Thus, based on mutants pΔ1 and pΔ3, we have identified a region important for stability between nucleotides 121306 and 121359. On the other hand, the region around nucleotide 121395 (where the *Bam*HI site was created in pBam) also appears to play a role in stability of the 2-kb LAT.

Defining the elements responsible for 2-kb LAT stability by limited mutagenesis. The region conferring stability was further investigated by creating smaller deletions, substitutions, or insertions in the last 110 nucleotides of the LAT intron (Fig. 5B). After transfection into Cos-1 cells, the LAT RNA produced by these mutants was analyzed by Northern blotting. In contrast to the first set of deletions, these deletions were small; therefore, a probe hybridizing simultaneously to the intron and exons could be used without resulting in an overlap of the intron and exons bands (Fig. 7). Again, the wt construct was used as a control, showing all three RNAs: primary transcript, accumulating intron, and mature exons (Fig. 7, lane 1); and pBam, as before, showed a reduced amount of intron (lane 2). The pΔG mutant was the only one in this panel to show accumulation of the LAT intron (lane 5); all the other mutants produced very low or undetectable level of intron. A quantification of the stability of these introns from calculations of the intron/exon ratio from three independent transfection experiments is shown in Fig. 8A. Again, pBam scored 60% of stability compared to the wt. The small deletion of pΔG did not affect stability, although the wt branch point was deleted in this construct. The creation of a mammalian consensus branch site in pCons dramatically reduced the stability of the 2-kb LAT intron, as did the deletion of the corresponding sequence in pΔA (Fig. 7, lanes 3 and 4). Similarly, a yeast consensus branch site introduced into pBam (mutant pY+ [lane 9]) resulted in the complete disappearance of the intron. Interestingly, the insertion of the same sequence in the opposite orientation (where no consensus branch site was introduced [24]) in pY−

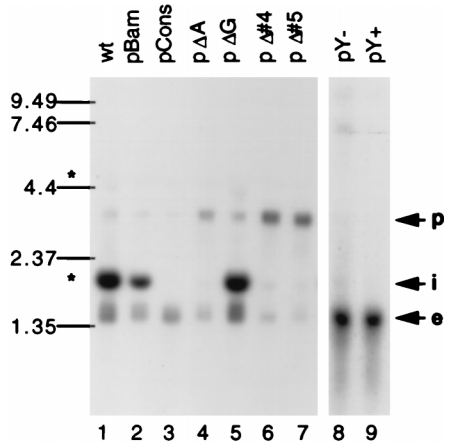

FIG. 7. Northern blot of LAT RNA. Total RNA from Cos-1 cells transfected with different constructs expressing wt (lane 1) or mutated (lanes 2 to 9) LATs hybridized with a probe detecting all primary transcripts (p), introns (i), and exons (e). RNA was collected 40 h posttransfection. The molecular size markers (in kilobases), as well as 28S and 18S rRNAs (asterisks), are indicated on the left.

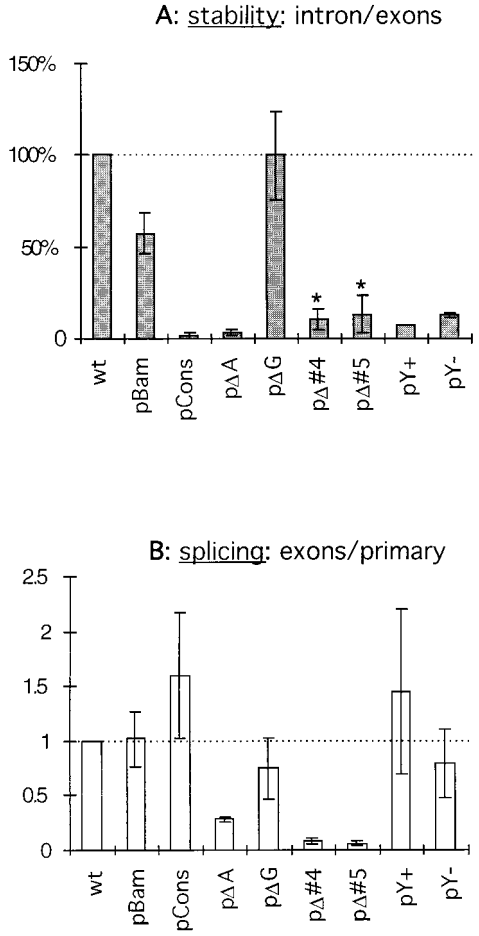

FIG. 8. Stability and splicing efficiency. Bands from the Northern blot presented in Fig. 7 as well as blots resulting from two other independent transfections were quantified. (A) The relative stability of the mutated introns is assessed by the ratio of intron to exons and expressed as percentage of the wt 2-kb LAT intron stability. Asterisks indicate introns produced after inefficient splicing. (B) The splicing efficiency is expressed by the ratio of exons to primary transcript. This ratio has been arbitrarily set to 1 for the wt construct. A low ratio reflects an inefficient splicing. Error bars show ±1 standard deviation.

also created an unstable intron (lane 8). Although the stability of the intron from pΔ4 and pΔ5 was significantly reduced, these mutants appeared to be impaired in splicing (lanes 6 and 7).

Relationship between splicing efficiency and intron stability. The major product of the pCons construct, in which a mammalian consensus branch site was created, was a mature transcript made of the spliced exons (Fig. 7, lane 3). In contrast, mutants pΔ4 and pΔ5 showed mainly an accumulation of the primary transcripts and produced only a limited amount of splicing products (lanes 6 and 7). To quantify the splicing efficiency of the different mutants, the ratio of the intensity of the mature exon band over the primary transcript band was calculated and set to 1 for the wt LAT construct (Fig. 8B). Since the stability of the primary transcript itself might be affected by the mutation, these numbers could give only an estimation of splicing efficiency. It appeared that splicing of pBam, pΔG, and pY− was as effective as that of the wt construct. Mutants carrying a consensus branch point (pCons and pY+) had a slightly increased efficiency of splicing, although their introns did not accumulate. The 8-base deletion in pΔA induced a reduction of 70% in splicing efficiency, whereas deletions in pΔ4 and pΔ5 had a more drastic effect and decreased splicing to 10% or less of the wt level.

Selection of branch points in mutant LATs. Evidence that the branch point of the 2-kb LAT is unique (58) and more resistant to enzymatic debranching (37) indicates that it may play an important role in conferring stability to the intron. Although deletion of the 2-kb LAT branch point and surrounding nucleotides in pΔG did not directly alter LAT stability, it was important to determine how different mutations influencing LAT stability would affect branching.

The branch RT-PCR method coupled with sequencing, described previously (58), was used to map the branch points of different mutants. The RT-PCR results are presented in Fig. 9, and the identified branch sites are presented in Fig. 10. For the wt construct, two PCR products of about 250 and 300 bp were identified (Fig. 9, lanes 1 and 4) and sequenced. The top band indicated the LAT branch point at the guanosine (position 121344) previously identified in transfections and in HSV-1 F-infected cultured cells or latently infected ganglia (58). The lower band may be due to a mispriming of the primer used for cDNA synthesis at nucleotide 121283, because of its sequence similarity in this region to the 5′ end of the intron (58). However, we cannot rule out the possibility that branching at that site also occurred. In the case of the pCons mutant, containing a mammalian consensus branch site (CACUGAC; branch point nucleotide underlined) and leading to the production of an unstable intron, a different PCR product was amplified (Fig. 9, lane 3). Sequencing revealed a branch point at the expected consensus site at position 121394 of pCons (Fig. 10). The construct pBam, which showed a partially reduced intron stability, also had an intermediate pattern of bands amplified in this RT-PCR experiment. In addition to the two bands seen with the wt construct, a third, slowly migrating band was visible in the gel (Fig. 9, lane 2). It appeared that the wt G nucleotide (position 121344) was still utilized but that a downstream branch region was also utilized in some introns at positions 121439 to 121441 (AUCCUUC). This region is also used for branching of the intron produced by pY− (derived from pBam

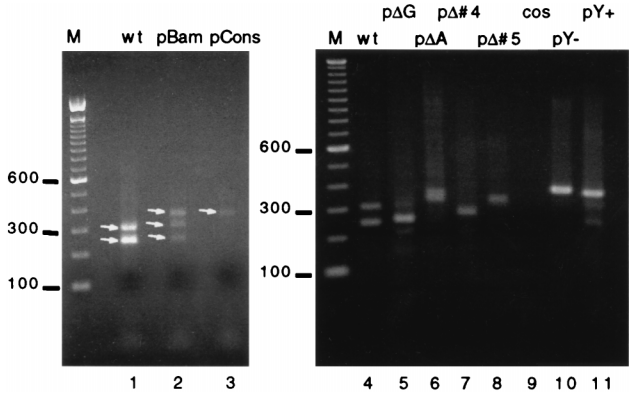

FIG. 9. RT-PCR mapping of the branch nucleotides. Gene-specific cDNA was synthesized with the degenerate oligonucleotide "Branch" as the primer from total RNA of transfected cells. Then amplification by PCR was performed with primers PFPML and PREND. Total RNA from cells transfected with wt and mutant constructs was used as the template. RNA from nontransfected cells was used as the negative control (cos). RT-PCR products were separated on a 2% agarose gel. The major bands of each reaction (indicated by arrows on the left panel only) were purified and cloned. Several clones corresponding to each band were grown and sequenced. M represents the 100-bp DNA ladder used as the molecular weight marker.

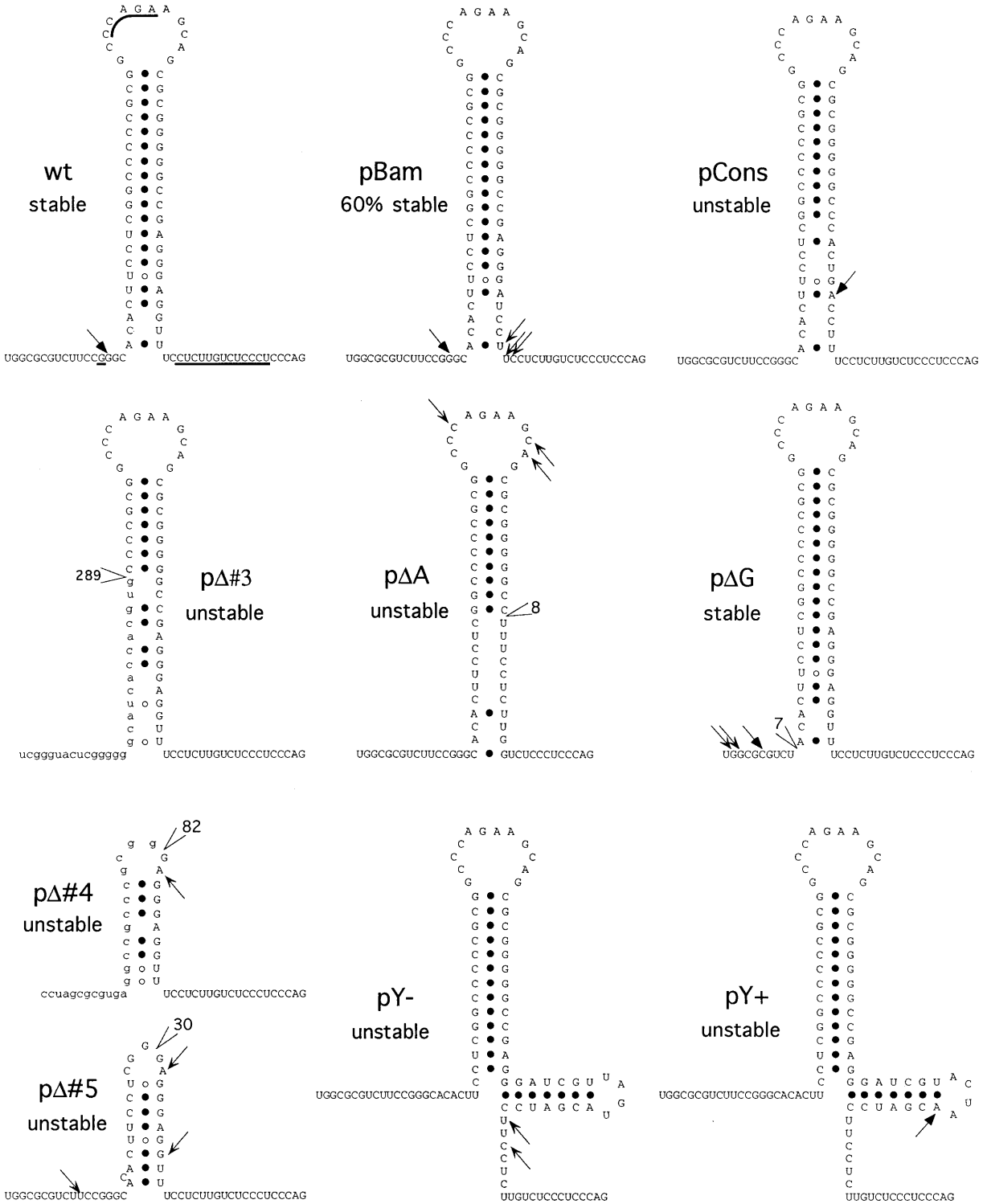

FIG. 10. Models of the 3′ end of the LAT introns. The wt sequence and putative structure are shown (wt) and compared to those of mutated LATs. For clarity, the putative structure of the mutant LATs is based on the wt LAT model, without taking newly generated structures into account (especially for mutants pΔ3, pΔ4, and pΔ5, in which the overall sequence in this region is altered). The positions and numbers of deleted nucleotides are indicated. Underlined bases in the wt model are changed between the HSV-1 and HSV-2 LAT (27). Small capital letters indicate upstream sequences brought into this region by the larger deletions of pΔ3 and pΔ4. Branch points are indicated by arrows (not determined for pΔ3). Full arrows indicate branch nucleotides in wt or consensus sites. Open arrows show alternative multiple branch points used by some mutants.

by the addition of a yeast consensus branch point in the wrong orientation at the *Bam*HI site) (Fig. 9, lane 10, Fig. 10).

The related clone, pY+ carrying a yeast consensus branch point sequence (UACUAAC) at the *Bam*HI site, preferentially used this consensus site for branching (Fig. 10). For pΔ4 and pΔ5, with deletions in the hairpin, splicing was impaired but the introns also displayed alternative branch point nucleotides in this area without strong preferences (Fig. 9, lanes 7 and 8; Fig. 10). In mutant pΔA, with an 8-base deletion immediately upstream of the polypyrimidine tract, the branch point was also relocated to different sites in the loop of the postulated hairpin (Fig. 10). In contrast to all the other mutants analyzed, pΔG displayed RT-PCR bands similar to the wt bands, although with differing intensities. The lower band is due to the mispriming at nucleotide 121283 as observed for the wt construct. Sequencing of the higher band indicated that branching occurred around the location used by the wt relative to the hairpin. However, due to the deletion, the branch point is now different (Fig. 10; pΔG; UGGCGCG). A summary of the different branch points of these mutants is shown on a model of the putative RNA secondary structure located at the 3′ end of the 2-kb LAT intron (Fig. 10).

DISCUSSION

The structures of the latency-associated gene products, RNA or protein, as well as their functions, remain largely unknown. Because there is no well-characterized functional agent for the LAT gene, studies have been based on HSV-1 deletion mutants unable to express LAT (3, 5, 22, 26, 33, 49, 53). Most of these mutants bear deletions in and around the LAT promoter region, directly affecting transcription. Among LAT-negative mutants studied previously, the TB1 virus is unusual in that it contains a mutation that does not directly affect the LAT promoter (4). The TB1 mutation consists of a deletion and insertion of foreign DNA in the middle of the 2-kb LAT sequence. Surprisingly, no 2-kb LAT can be detected in TB1-infected cells or latently infected murine trigeminal ganglia (4).

TB1 does make a stable intron. In the present study, we have used eucaryotic expression system for the 2-kb LAT to determine how its expression is altered in the TB1 virus. The RNA produced by constructs pΔHpa and pHλ+ showed that neither the deletion of 168 nucleotides in the middle of the 2-kb LAT nor the insertion of a foreign sequence in this molecule is sufficient to alter the production of a stable LAT intron. However, the oriented lambda phage sequence in the HSV-1 TB1 mutant contains regions acting as splice donor and splice acceptor sites. The addition of these sites allows processing of a new lambda-derived exon that disrupts the 2-kb LAT intron in TB1. As a result, the stable 2-kb LAT cannot be detected.

However, the 2-kb LAT is replaced by smaller introns, the farthest 3′ of which can be detected by Northern blot analysis (4). It was previously postulated that this RNA arose from a promoter activity lying within the lambda DNA insert (4). The present RT-PCR data show that the primary transcript from TB1 contains LAT exon 1 and indicate that the 0.95-kb RNA detected by Northern blotting is a stable intron (Fig. 1 and 4). The lack of detection of this 0.95-kb RNA in latently infected murine trigeminal ganglia (4) remains to be explained. Another mutant virus, 17N/H, carries the same lambda sequence insertion replacing a larger *Not*I-*Hpa*I fragment of the LAT locus (3). Most of the LAT promoter, the whole of exon 1, and the first half of the 2-kb LAT intron are missing from this virus. However, the lambda insert, its 3′ boundary with viral sequences, and the downstream region of the 2-kb LAT in 17N/H are comparable to those of TB1. Similar to TB1, this viral mutant also produces a 0.95-kb LAT RNA which maps directly downstream of the lambda insert without significant 5′ extension into the phage sequence (3). However, in the case of 17N/H, the promoter and the primary transcript from which this putative intron is spliced have not been identified.

Mutant virus TB1 does not display any phenotypic difference from its parental strain (HFEM) as far as growth or reactivation kinetics are concerned (4). If a yet undiscovered protein translated from the mature LAT mRNA is the active agent of the LAT gene, alterations of splicing between exons 1 and 2 do not significantly affect its production or activity. Since the 2-kb LAT is an unusually stable RNA, it has been proposed to be active, itself, as a negative regulator of ICP0 expression (16, 52). This antisense inhibition mechanism is reasonable because ICP0 mRNA is transcribed from the opposite strand and overlaps with 1 kb of the 3′ end of the 2-kb LAT RNA (Fig. 1A). The truncated, and still stable, 0.95-kb LAT intron from TB1 retains the complete region antisense with respect to the ICP0 transcript. Thus, the absence of a phenotype for TB1 would seem consistent with the antisense hypothesis. In contrast to TB1, the 17N/H mutant, with a large deletion removing all of the LAT gene 5′ of the TB1 substitution, shows slow kinetics of reactivation and a small-plaque phenotype (3). Since both mutants produce a similar 0.95-kb LAT, the cause of the difference in phenotype (3) appears to lie in the region upstream of the second half of 2-kb LAT, consistent with recent observations (33). This suggests that antisense inhibition of ICP0, if it occurs, does not explain these phenotypes.

The 2-kb LAT stability maps to its 3′ 100 nucleotides. Beside its functional aspects, the 2-kb LAT is interesting because it is an unusually stable intron. To identify the LAT sequence elements required for stability, we analyzed a panel of mutated LAT introns expressed in tissue culture. We have shown that TB1 does express mLAT and a truncated stable LAT intron from a splice donor site in the lambda insert (Fig. 2 and 4). The presence of this truncated stable intron, from TB1 or from the related pHλ− construct, indicates that the 3′ half of the 2-kb LAT by itself contains the necessary elements to confer stability to the LAT intron in tissue culture. The 5′ end of the TB1 0.95-kb intron generated at the lambda splice donor site is different from the wt 2-kb LAT with the exception of the first 3 bases (GTA). This indicates that sequences at the 5′ end of the intron, other than the GTA involved in branching to form the lariat, are not crucial for LAT stability in infected and transfected cultured cells.

The panel of LAT deletion plasmids analyzed in the second part of this study identifies the region conferring stability to the last 100 bp of the 2-kb LAT intron. The use of mutations Δ1 and Δ3 showed that the region between nucleotides 121306 and 121359, encompassing the wt branch point at position 121344 (58) and part of a putative hairpin structure (Fig. 10), appeared to be important for stability of the LAT intron. In addition, the 3-nucleotide substitution in pBam significantly affects LAT stability, indicating that the 5′ end of the polypyrimidine tract is also involved in the stability of the 2-kb LAT.

Location of the nonconsensus branch point correlates with intron stability. The 2-kb LAT branch point nucleotide (a guanosine [58]) is unusual because branch point nucleotides are normally adenosines (35). In vitro, guanosine and cytosine branch points are known to be resistant to debranching (1, 24), a step opening the way to intron degradation (8). In the panel of mutants generating an unstable intron, the four nucleotides (G, U, A, and C) in nonconsensus sequences can be used as a branch points (Fig. 10). Despite having nonadenosine branch points, these introns were rapidly degraded and did not accu-

mulate. For the mutant which can utilize a G branch point and produce an unstable intron, it should be pointed out that this mutant, pΔ5, does not splice efficiently and uses several different nucleotides as branch points; therefore, the frequency at which a guanosine is used as a branch point in unstable introns is low. Two mutations introduce a consensus branch point, from either yeast (pY+) or mammalian (pCons) origin. In both cases, the new consensus adenosine branch site is preferred over the wt LAT branch point; this selection correlates with the production of highly unstable introns. In pΔG, a 7-nucleotide deletion removes the wt branch point region, resulting in branching at guanosine and cytosine; despite these changes, this intron remains stable. In this pΔG mutant, the branch nucleotide and the surrounding sequence are modified but the location relative to the secondary structure is not changed. This indicates that the natural branch point region does not have to be conserved to ensure the stability of the 2-kb LAT.

The use of all four nucleotides as branch points in unstable introns and the deletion of the wt guanosine in a stable intron suggest that the stability of the 2-kb LAT intron is also determined by factors different from the branch point nucleotide. Interestingly, stable introns from wt and pΔG branches are in a specific location upstream of a putative hairpin structure; in contrast, unstable intron branch points are located downstream of or in the loop of the hairpin. The correlation between the stability and location of the branch point suggests a mechanism involving the RNA structure in the generation of the stable 2-kb LAT intron.

A putative hairpin structure influences the selection of a nonconsensus branch point. Hairpin structures are known to play important roles in stabilization of RNAs. They can bind specific proteins or build nuclease-resistant cores. The putative stem-loop structure in the tail of the 2-kb LAT may play a role in the stability of the LAT intron through either mechanism. However, its most interesting characteristic lies in its ability to influence branch point selection. As reported previously, there are no consensus mammalian branch point sites (YNYURAC) near the 3′ end of the 2-kb LAT intron (57, 58). Thus, the branching of the LAT intron has to occur at a nonconventional site. The suboptimal branch sequence (GAGGGAG) hypothesized by Wu et al. (57), which is located directly upstream of the polypyrimidine tract, is not used during wt LAT splicing (58). Structurally, this suboptimal branch point is located in the stem of a hairpin structure (Fig. 10), a location known to prevent efficient branching (20).

In the wt HSV-1 virus or wt construct, the nonconsensus branch point at position 121344 is highly preferred during the splicing of the 2-kb LAT. However, minor modifications at the base of the putative hairpin significantly reduce intron stability. The mutation in the pBam construct consists of a 3-base substitution at the base of the stem, which disrupts one G · C base pairing and extends the polypyrimidine tract by 2 nucleotides, without introducing a consensus branch point (Fig. 5B). The wt branch point is still used by this mutant, but a significant proportion of introns branch at the opposite side of the hairpin, at the 5′ end of the polypyrimidine tract (Fig. 10). The overall 60% stability of the pBam intron may reflect the selection of the branch point: 60% branching at the wt guanosine branch point giving a stable intron, and 40% branching at the polypyrimidine branch points resulting in unstable introns. A more extended mutation was engineered in the pBam-derived mutant pY− by the insertion of 12 nucleotides into the *Bam*HI site. In this mutant, branching does not occur at the wt branch point but occurs in the region downstream of the hairpin at the end of the polypyrimidine tract. The exclusive use of this region for branching leads to the production of an unstable intron.

Mutants pY+ and pY− differ by the presence (pY+) or absence (pY−) of a consensus branch point, but their putative hairpin structures are similar (Fig. 10). Both mutants produce an unstable intron, indicating that the specific hairpin structure plays a role in stability. However, these two mutants display different branching preferences. While pY+ uses the consensus branch point, pY− branches at the end of the polypyrimidine tract, indicating that the presence of a consensus branch point sequence in this region is not necessary to destabilize the 2-kb LAT. However, when present, a consensus branch point sequence appears to be strongly favored.

Deletions affecting either RNA strand involved in the stem of the hairpin (pΔA, pΔ3, pΔ4, and pΔ5) alter more drastically the base pairing and the length of the stem. This decrease in the stability of the hairpin correlates with relocation of the branch point in this region without strong preferences. In addition, none of these mutants generate a stable intron.

Taken together, these results suggest a strong correlation between the overall stability of the 2-kb LAT and the putative hairpin depicted in Fig. 10. This correlation may be mediated through the ability of the stem-loop to influence the selection and location of the nonconsensus branch point used to splice the 2-kb LAT.

The putative hairpin is necessary for efficient splicing. Mutations affecting the base of the stem-loop structure (pBam and pY−) have no significant effect on the splicing efficiency (Fig. 8B). In the case of mutations limited to the middle-stem region, the negative influence on splicing is greater; for instance, pΔA reduces the splicing efficiency by 70%. When the hairpin is altered in the upper stem region and in the loop (pΔ4 and pΔ5), leading to a different structure (Fig. 10), the splicing efficiency of this intron is reduced to less than 10% of the wt efficacy. These observations stress the importance of the role of this structure during splicing. It is known that availability and proper selection of branch points are important for efficient splicing. Mutations or deletions of branch points usually lead to exon skipping due to lack of recognition of the mutated intron (21, 36). Complex mechanisms involved in branch point selection include the recognition of the consensus sequence as well as the surrounding area (14), the length and type of polypyrimidine tract (32, 39), and the presence of secondary structures (20). In the case of 2-kb LAT, this selection is influenced by a putative RNA secondary structure at the 3′ end of the intron. The mechanism of branch point identification appears to be quite efficient, since the presence of a strong consensus site in this sequence increased the splicing efficiency by only 1.5- to 2-fold (Fig. 8B). On the other hand, deletion of the loop of the hairpin decreases the splicing efficiency by 10 fold (Fig. 8B), probably because no branch points can be identified in these introns. Thus, in the absence of a consensus branch point, the putative structure would allow the recognition of a nonconsensus branch point necessary for the splicing of the 2-kb LAT.

A similar hairpin can be formed in the HSV-2 LAT intron but not in other stable introns. The 3′-end sequence of HSV-2 2.3-kb LAT is able to form the same putative secondary structure as HSV-1 and also does not have a consensus branch point (27). The stem of the hairpin is identical to the HSV-1 counterpart, and divergence is found mainly in the polypyrimidine tract and in the loop (Fig. 10). Thus, one can hypothesize a similar branch point selection mechanism leading to the stability of the HSV-2 LAT intron.

Recently, a stable intron from the HSV-1 ICP0 gene was described (6). Although it is not clear whether the stability of

the ICP0 intron is equivalent to that of the LAT intron, they both seem to utilize different mechanisms for stability. This intron uses four different splice acceptor sites within 300 bp. A consensus branch point is associated with the most upstream splice acceptor site, whereas sequences with six-of-seven-base matches to the consensus (YNYURAC) could be found near the acceptor site for each other intron. Another stable intron spliced from the constant region of the T-cell receptor β locus accumulates in T cells as a lariat (34). In that case, five of seven bases matched the consensus branch site and no strong stem-loop structure could be detected at the 3′ end of this intron. A short sequence (AUUUUC) at the end of the polypyrimidine tract has been proposed to be involved in the stability of this intron based on comparisons with other similar stable introns (34). This U-rich sequence is absent from the 3′ end of the 2-kb LAT intron. By sequence comparison with these other stable introns, the 2-kb LAT appears to use a different mechanism to increase its stability.

In conclusion, our results indicate that splicing of the HSV 2-kb LAT in tissue culture appears to be achieved by the selection of a nonconsensus branch site, whose location is driven by a strong RNA secondary structure. Conservation of this stem-loop structure is required to direct the branch site localization and recognition, which lie at the origin of HSV 2-kb LAT splicing and stability.

ACKNOWLEDGMENTS

We are grateful to Timothy Block (Thomas Jefferson University Medical School) for supplying the pNF1 plasmid and for helpful comments. We appreciate the excellent technical support provided by Jennifer Unsell and the members of the Nucleic Acids Facility of the Wistar Institute.

C.K. was supported by a fellowship from the Swiss National Science Foundation. J.M.Z. was supported by NIH training grant AI07325. This work was supported by Public Health Service grant NS33768 from the NIH.

REFERENCES

1. **Arenas, J., and J. Hurwitz.** 1987. Purification of a RNA debranching activity from Hela cells. J. Biol. Chem. **262:**4274–4279.
2. **Ausubel, F. M., R. Brent, R. E. Kingston, D. D. Moore, J. A. Smith, J. G. Seidmen, and K. Struhl.** 1987. Current protocols in molecular biology. Greene Publishing Associates and Wiley-Interscience, New York, N.Y.
3. **Block, T. M., S. L. Deshmane, J. Masonis, J. Maggioncalda, T. Valyi-Nagy, and N. W. Fraser.** 1992. An HSV LAT null mutant reactivates slowly from latent infection and makes small plaques on CV-1 monolayers. Virology **192:**618–630.
4. **Block, T. M., J. G. Spivack, I. Steiner, S. Deshmane, M. T. McIntosh, R. P. Lirette, and N. W. Fraser.** 1990. A herpes simplex virus type 1 latency-associated transcript mutant reactivates with normal kinetics from latent infection. J. Virol. **64:**3417–3426.
5. **Bloom, D. C., J. M. Hill, G. Devi-Rao, E. K. Wagner, L. T. Feldman, and J. G. Stevens.** 1996. A 348-base-pair region in the latency-associated transcript facilitates herpes simplex virus type 1 reactivation. J. Virol. **70:**2449–2459.
6. **Carter, K. L., and B. Roizman.** 1996. Alternatively spliced mRNAs predicted to yield frame-shift proteins and stable intron 1 RNAs of the herpes simplex virus 1 regulatory gene alpha 0 accumulate in the cytoplasm of infected cells. Proc. Natl. Acad. Sci. USA **93:**12535–12540.
7. **Castanotto, D., and J. J. Rossi.** 1992. Small sequence insertions within the branch point region dictate alternative sites of lariat formation in a yeast intron. Nucleic Acids Res. **20:**6649–6655.
8. **Chapman, K. B., and J. D. Boeke.** 1991. Isolation and characterization of the gene encoding yeast debranching enzyme. Cell **65:**483–492.
9. **Deatly, A. M., J. G. Spivack, E. Lavi, and N. W. Fraser.** 1987. RNA from an immediate early region of the HSV-1 genome is present in the trigeminal ganglia of latently infected mice. Proc. Natl. Acad. Sci. USA **84:**3204–3208.
10. **Deatly, A. M., J. G. Spivack, E. Lavi, D. R. O'Boyle II, and N. W. Fraser.** 1988. Latent herpes simplex virus type 1 transcripts in peripheral and central nervous system tissues of mice map to similar regions of the viral genome. J. Virol. **62:**749–756.
11. **Devi-Rao, G. B., S. A. Goodart, L. M. Hecht, R. Rochford, M. A. Rice, and E. K. Wagner.** 1991. Relationship between polyadenylated and nonpolyadenylated herpes simplex virus type 1 latency-associated transcripts. J. Virol. **65:**2179–2190.
12. **Dobson, A. T., F. Sederati, G. Devi-Rao, J. Flanagan, M. J. Farrell, J. G. Stevens, E. K. Wagner, and L. T. Feldman.** 1989. Identification of the latency-associated transcript promoter by expression of rabbit beta-globin mRNA in mouse sensory nerve ganglia latently infected with a recombinant herpes simplex virus. J. Virol. **63:**3844–3851.
13. **Doerig, C., L. I. Pizer, and C. L. Wilcox.** 1991. An antigen encoded by the latency-associated transcript in neuronal cell cultures latently infected with herpes simplex virus type 1. J. Virol. **65:**2724–2727.
14. **Dominski, Z., and R. Kole.** 1994. Identification and characterization by antisense oligonucleotides of exon and intron sequences required for splicing. Mol. Cell. Biol. **14:**7445–7454.
15. **Estes, P. A., N. E. Cooke, and S. A. Liebhaber.** 1992. A native RNA secondary structure controls alternative splice-site selection and generates two human growth hormone isoforms. J. Biol. Chem. **267:**14902–14908.
16. **Farrell, M. J., A. T. Dobson, and L. T. Feldman.** 1991. Herpes simplex virus latency-associated transcript is a stable intron. Proc. Natl. Acad. Sci. USA **88:**790–794.
17. **Fraser, N. W., T. M. Block, and J. G. Spivack.** 1992. The latency-associated transcripts of herpes simplex virus: RNA in search of function. Virology **191:**1–8.
18. **Fraser, N. W., J. G. Spivack, Z. Wroblewska, T. Block, S. L. Deshmane, T. Valyi-Nagy, R. Natarajan, and R. Gesser.** 1991. A review of the molecular mechanism of HSV-1 latency. Curr. Eye Res. **10**(Suppl.)**:**1–14.
19. **Gaur, R. K., J. Valcarcel, and M. R. Green.** 1995. Sequential recognition of the pre-mRNA branch point by U2AF65 and a novel spliceosome-associated 28-kDa protein. RNA **1:**407–417.
20. **Goguel, V., Y. Wang, and M. Rosbash.** 1993. Short artificial hairpins sequester splicing signals and inhibit yeast pre-mRNA splicing. Mol. Cell. Biol. **13:**6841–6848.
21. **Hara, T., M. Ichihara, M. Takagi, and A. Miyajima.** 1995. Interleukin-3 (IL-3) poor-responsive inbred mouse strains carry the identical deletion of a branch point in the IL-3 receptor alpha subunit gene. Blood **85:**2331–2336.
22. **Hill, J. M., F. Sederati, R. T. Javier, E. K. Wagner, and J. G. Stevens.** 1990. Herpes simplex virus latent phase transcription facilitates in vivo reactivation. Virology **174:**117–125.
23. **Horton, R. M.** 1993. In vitro recombination and mutagenesis of DNA, p. 251–261. *In* B. A. White (ed.), PCR protocols: current methods and applications. Humana Press Inc., Totowa, N.J.
24. **Jacquier, A., and M. Rosbash.** 1986. RNA splicing and intron turnover are greatly diminished by a mutant yeast branch point. Proc. Natl. Acad. Sci. USA **83:**5835–5839.
25. **Kuivenhoven, J. A., H. Weibusch, P. H. Pritchard, H. Funke, R. Benne, G. Assmann, and J. J. P. Kastelein.** 1996. An intronic mutation in a lariat branchpoint sequence is a direct cause of an inherited human disorder (fish-eye disease). J. Clin. Invest. **98:**358–364.
26. **Leib, D. A., C. L. Bogard, M. Kosz-Vnenchak, K. A. Hicks, D. M. Coen, D. M. Knipe, and P. A. Schaffer.** 1989. A deletion mutant of the latency-associated transcript of herpes simplex virus type 1 reactivates from the latent infection. J. Virol. **63:**2893–2900.
27. **McGeoch, D. J., C. Cunningham, G. McIntyre, and A. Dolan.** 1991. Comparative sequence analysis of the long repeat regions and adjoining parts of the long unique regions in the genomes of herpes simplex viruses types 1 and 2. J. Gen. Virol. **69:**1531–1574.
28. **McGeoch, D. J., M. A. Dalrymple, A. J. Davison, A. Dolan, M. C. Frame, D. McNab, L. J. Perry, J. E. Scott, and P. Taylor.** 1988. The complete DNA sequence of the long unique region in the genome of herpes simplex virus type 1. J. Gen. Virol. **69:**1531–1574.
29. **Mitchell, W. J., R. P. Lirette, and N. W. Fraser.** 1990. Mapping of low abundance latency associated RNA in the trigeminal ganglia of mice latently infected with herpes simplex virus type 1. J. Gen. Virol. **71:**125–132.
30. **Moore, M. J., C. C. Query, and P. A. Sharp.** 1993. Splicing of precursors to messenger RNAs by the spliceosome, p. 1–30. *In* R. F. Gesteland and J. F. Atkins (ed.), The RNA world. Cold Spring Harbor Laboratory Press, Cold Spring Harbor, N.Y.
31. **Nam, K., R. H. Hudson, K. B. Chapman, K. Ganeshan, M. J. Damha, and J. D. Boeke.** 1994. Yeast lariat debranching enzyme. Substrate and sequence specificity. J. Biol. Chem. **269:**20613–20621.
32. **Norton, P. A.** 1994. Polypyrimidine tract sequences direct selection of alternative branch sites and influence protein binding. Nucleic Acids Res. **22:** 3854–3860.
33. **Perng, G. C., H. Ghiasi, S. M. Slanina, A. B. Nesburn, and S. L. Wechsler.** 1996. The spontaneous reactivation function of the herpes simplex virus type 1 LAT gene resides completely within the first 1.5 kilobases of the 8.3-kilobase primary transcript. J. Virol. **70:**976–984.
34. **Qian, L., M. N. Vu, M. Carter, and M. F. Wilkinson.** 1992. A spliced intron accumulates as a lariat in the nucleus of T cells. Nucleic Acids Res. **20:**5345–5350.
35. **Query, C. C., S. A. Strobel, and P. A. Sharp.** 1996. Three recognition events at the branch-site adenine. EMBO J. **15:**1392–1402.
36. **Ris-Stalpers, C., M. C. Verleun-Mooijman, T. J. P. d. Blaeij, H. J. Degenhart, J. Trapman, and A. O. Brinkmann.** 1994. Differential splicing of human androgen receptor pre-mRNA in X-linked Reifenstein syndrome, because of

a deletion involving a putative branch site. Am. J. Hum. Genet. **54:**609–617.
37. **Rodahl, E., and L. Haarr.** 1997. Analysis of the 2-kilobase latency-associated transcript expressed in PC12 cells productively infected with herpes simplex virus type 1: evidence for a stable, nonlinear structure. J. Virol. **71:**1703–1707.
38. **Roizman, B., and A. E. Sears.** 1987. An inquiry into the mechanisms of herpes simplex virus latency. Annu. Rev. Microbiol. **41:**543–571.
39. **Roscigno, R. F., M. Weiner, and M. A. Garcia-Blanco.** 1993. A mutational analysis of the polypyrimidine tract of introns: effects of sequence differences in pyrimidine tracts on splicing. J. Biol. Chem. **268:**11222–11229.
40. **Saini, K. S., I. C. Summerhayes, and P. Thomas.** 1990. Molecular events regulating messenger RNA stability in eukaryotes. Mol. Cell. Biochem. **96:** 15–23.
41. **Sawtell, N. M., and R. L. Thompson.** 1992. Herpes simplex virus type 1 latency-associated transcription unit promotes anatomical site-dependent establishment and reactivation from latency. J. Virol. **66:**2157–2169.
42. **Schang, L. M., A. Hossain, and C. Jones.** 1996. The latency-related gene of bovine herpesvirus 1 encodes a product which inhibits cell cycle progression. J. Virol. **70:**3807–3814.
43. **Solnick, D.** 1985. Alternative splicing caused by RNA secondary structure. Cell **43:**667–676.
44. **Spivack, J. G., and N. W. Fraser.** 1987. Detection of herpes simplex virus type 1 transcripts during latent infection in mice. J. Virol. **61:**3841–3847.
45. **Spivack, J. G., and N. W. Fraser.** 1988. Expression of herpes simplex virus type 1 (HSV-1) latency-associated transcripts in the trigeminal ganglia of mice during acute infection and reactivation of latent infection. J. Virol. **62:**1479–1485.
46. **Spivack, J. G., and N. W. Fraser.** 1988. Expression of herpes simplex virus type 1 (HSV-1) latency-associated transcripts and transcripts affected by the detection in the avirulent mutant HFEM: evidence for a new class of HSV-1 genes. J. Virol. **62:**3281–3287.
47. **Spivack, J. G., G. M. Woods, and N. W. Fraser.** 1991. Identification of a novel latency-specific splice donor signal within the herpes simplex virus type 1 2.0 kb latency-associated transcript (LAT): translation inhibition of LAT open reading frames by the intron within the 2.0 kb LAT. J. Virol. **65:**6800–6810.
48. **Staffa, A., and A. Cochrane.** 1994. The tat/rev intron of human immunodeficiency virus type 1 is inefficiently spliced because of suboptimal signals in the 3′ splice site. J. Virol. **68:**3071–3079.
49. **Steiner, I., J. G. Spivack, R. P. Lirette., S. M. Brown, A. R. MacLean, J. Subak-Sharpe, and N. W. Fraser.** 1989. Herpes simplex virus type 1 latency-associated transcripts are evidently not essential for latent infection. EMBO J. **8:**505–511.
50. **Steiner, I., J. G. Spivack, D. R. O'Boyle, E. Lavi, and N. W. Fraser.** 1988. Latent herpes simplex virus type 1 transcription in human trigeminal ganglia. J. Virol. **62:**3493–3496.
51. **Stevens, J. G.** 1989. Human herpesviruses: a consideration of the latent state. Microbiol. Rev. **53:**318–332.
52. **Stevens, J. G., E. K. Wagner, G. B. Devi-Rao, M. L. Cook, and L. T. Feldman.** 1987. RNA complementary to a herpes virus gene mRNA is prominent in latently infected neurons. Science **235:**1056–1059.
53. **Trousdale, M., I. Steiner, J. G. Spivack, S. L. Deshmane, S. M. Brown, A. S. MacLean, J. H. Subak-Sharpe, and N. W. Fraser.** 1991. Evidence that the herpes simplex virus type 1 latency-associated transcripts play a role in reactivation of latent infection in vivo. J. Virol. **65:**6989–6993.
54. **Wagner, E. K., G. Devi-Rao, L. T. Feldman, A. T. Dobson, Y. F. Zhang, J. M. Hill, W. M. Flanagan, and J. G. Stevens.** 1988. Physical characterization of the herpes simplex virus latency-associated transcript in neurons. J. Virol. **62:**1194–1202.
55. **Wagner, E. K., W. M. Flanagan, G. Devi-Rao, Y. F. Zhang, J. M. Hill, K. P. Anderson, and J. G. Stevens.** 1988. The herpes simplex virus latency-associated transcript is spliced during the latent phase of infection. J. Virol. **62:** 4577–4585.
56. **Whitley, R. J.** 1990. Herpes simplex viruses, p. 1843–1887. *In* B. N. Fields (ed.), Virology. Raven Press, New York, N.Y.
57. **Wu, T. T., Y. H. Su, T. M. Block, and J. M. Taylor.** 1996. Evidence that two latency-associated transcripts of herpes simplex virus type 1 are nonlinear. J. Virol. **70:**5962–5967.
58. **Zabolotny, J. M., C. Krummenacher, and N. W. Fraser.** 1997. The herpes simplex virus type 1 2.0-kilobase latency-associated transcript is a stable intron which branches at a guanosine. J. Virol. **71:**4199–4208.
59. **Zwaagstra, J., H. Ghiasi, S. M. Slanina, A. B. Nesburn, S. C. Wheatley, K. Lillycrop, J. Wood, D. S. Latchman, K. Patel, and S. L. Wechsler.** 1990. Activity of herpes simplex virus type 1 latency-associated transcript (LAT) promoter in neuron-derived cells: evidence for neuron specificity and for a large LAT transcript. J. Virol. **64:**5019–5028.